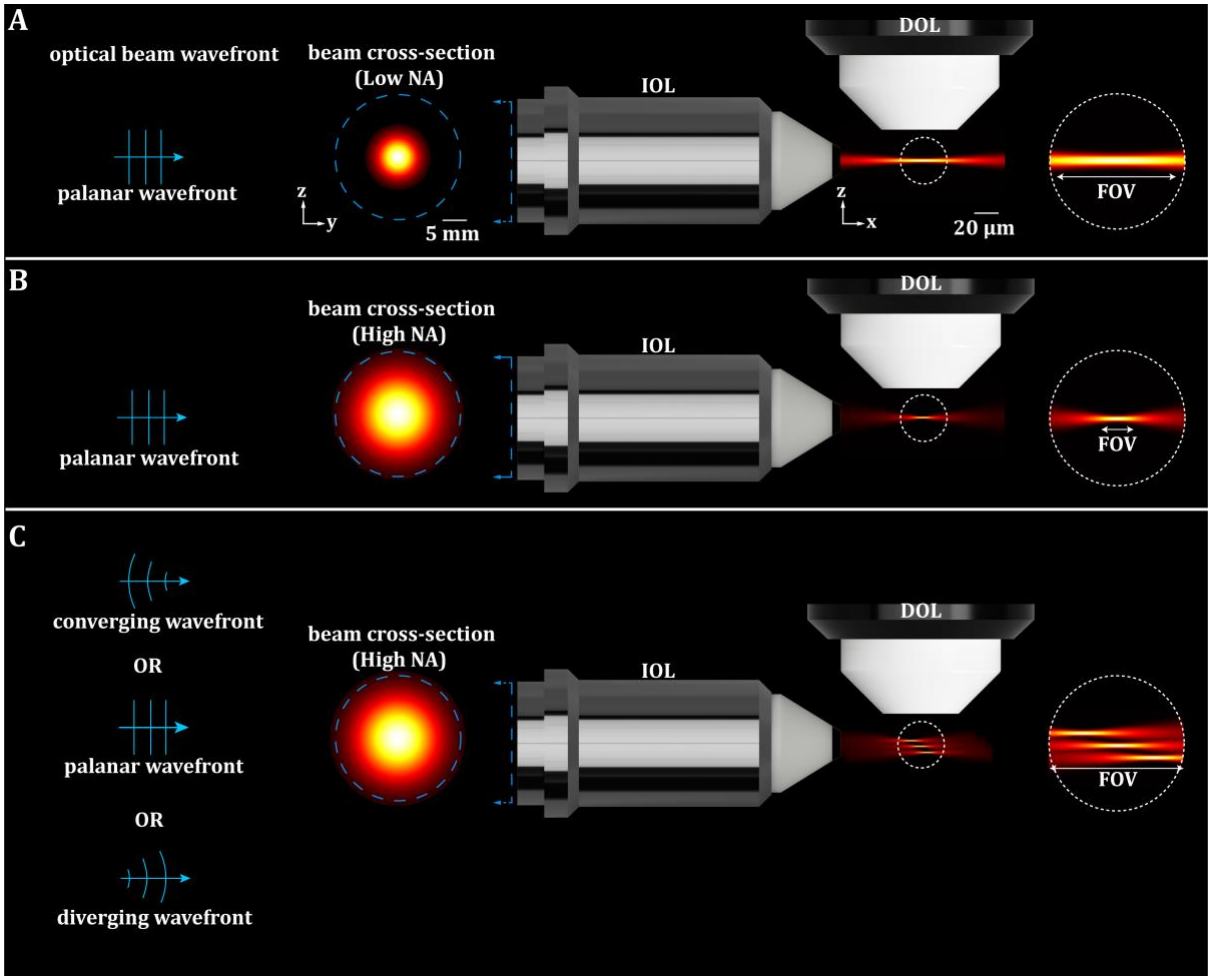

Fig. S1. Light sheet thickness and its effective field of view. The size of the light sheet at the sample plane is proportional to the diameter of the illumination beam at the rear pupil of the illumination objective lens(IOL). (A) A narrower diameter illumination beam at the IOL's rear pupil produces a thick centered beam with a wide field of view (FOV). (B) A greater diameter light beam at the IOL's rear pupil results in a thinner and smaller FOV at the sample plane. (C) By slightly changing the wavefront of the illumination beam in the IOL's rear pupil, the thin light sheet can be tilled over the broad FOV.

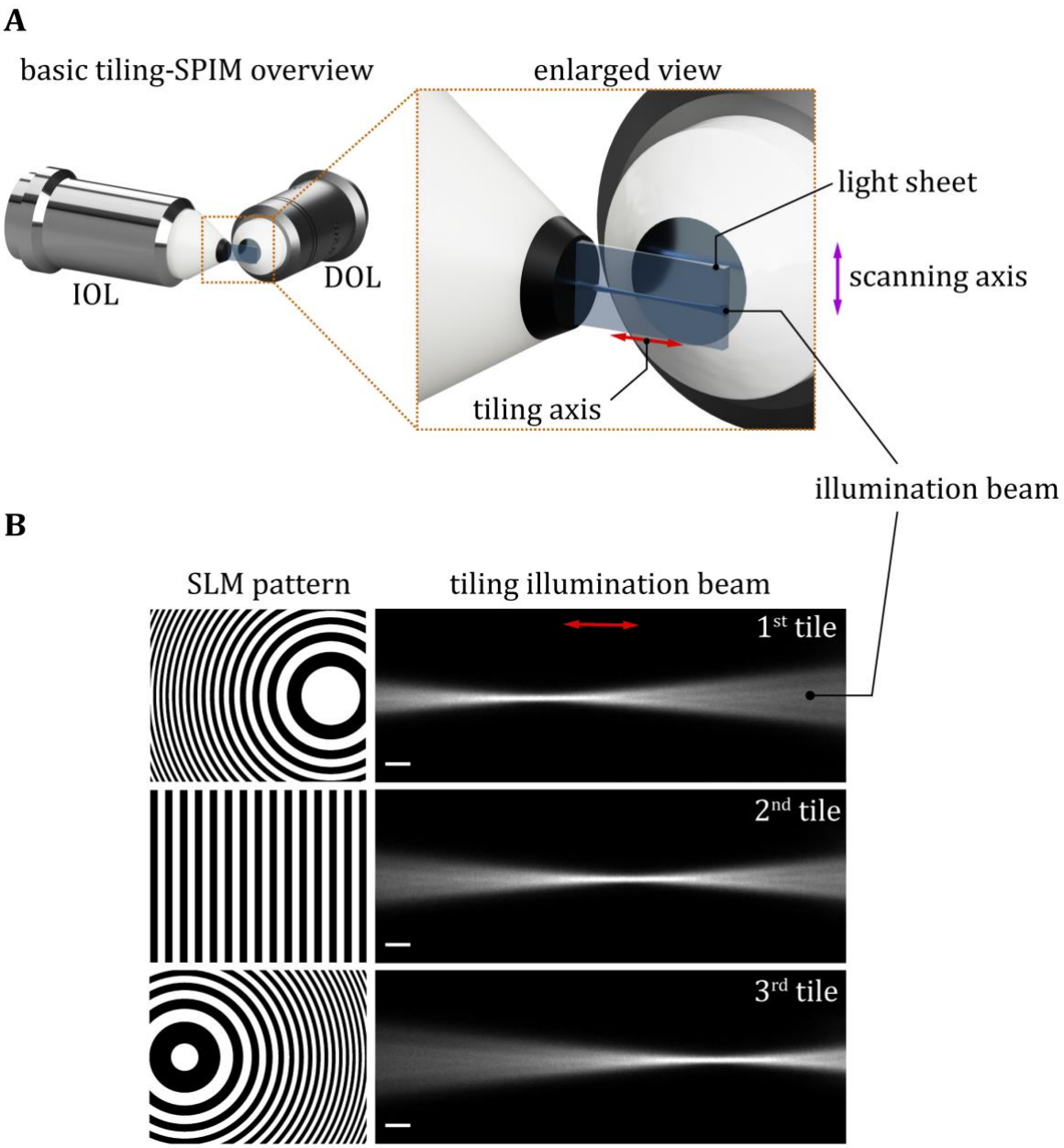

Fig. S2. The tiling technique is depicted in the SPIM simple setup. (A) The basic SPIM configuration with two objective lenses. (B) The left column depicts three distinct SLM patterns based on virtual lenses with various focal lengths, and the right column depicts the recorded the tiled illumination beams through the dye solution. Scale bars, 10 μm.

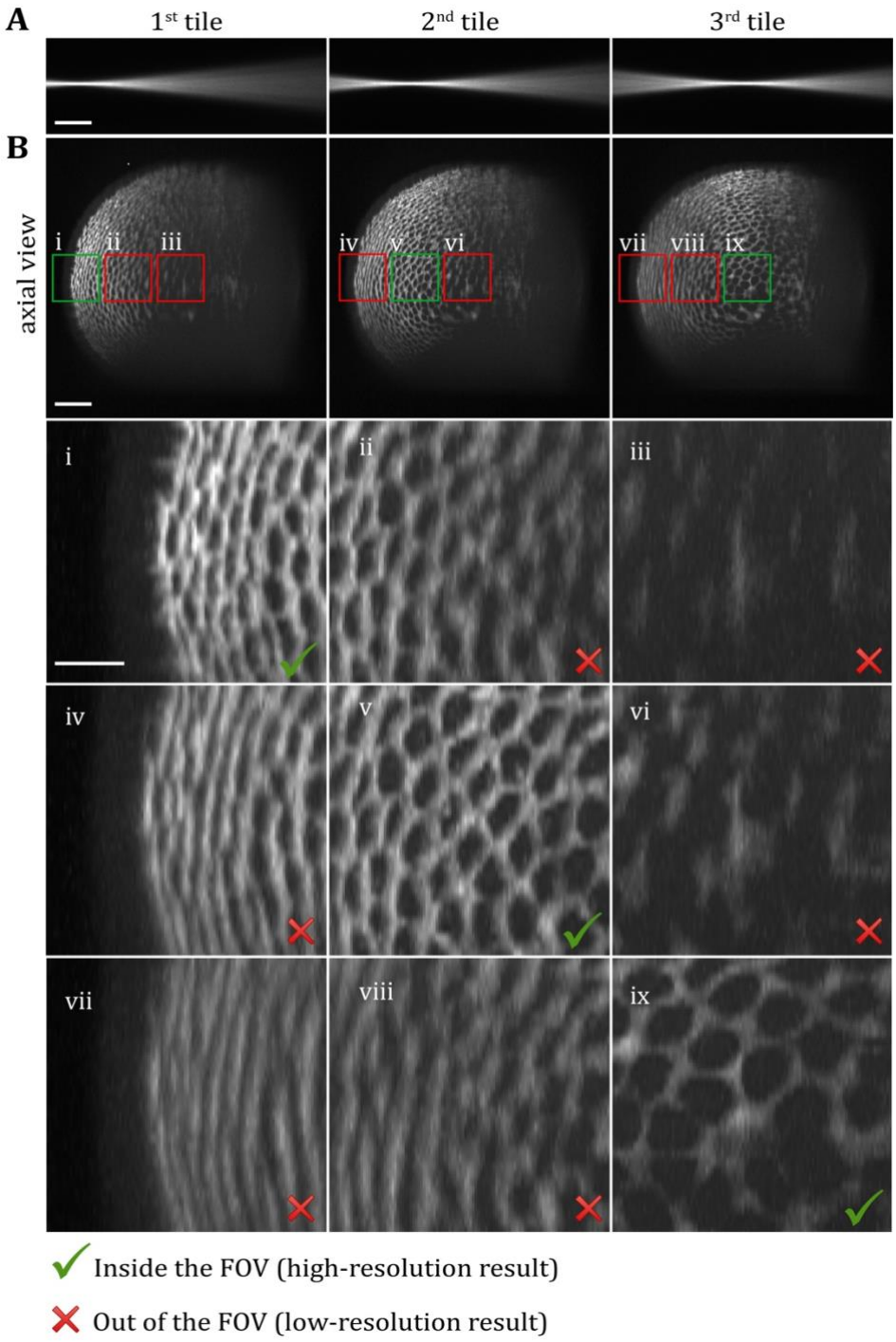

Fig. S3. The performance of the Basic tiling-SPIM with two objective lenses for imaging an opaque sample. (A) Tilled illumination beam through dye solution. (B) A reconstructed axial view of a recorded *Drosophila* embryo for each tiled light sheet is shown (A). The green marked area represented the maximum axial resolution on each tiled light sheet, which should be considered for the final image reconstruction. The scale bars for A and B are 30 μm and 10 μm for the subset images (i-ix).

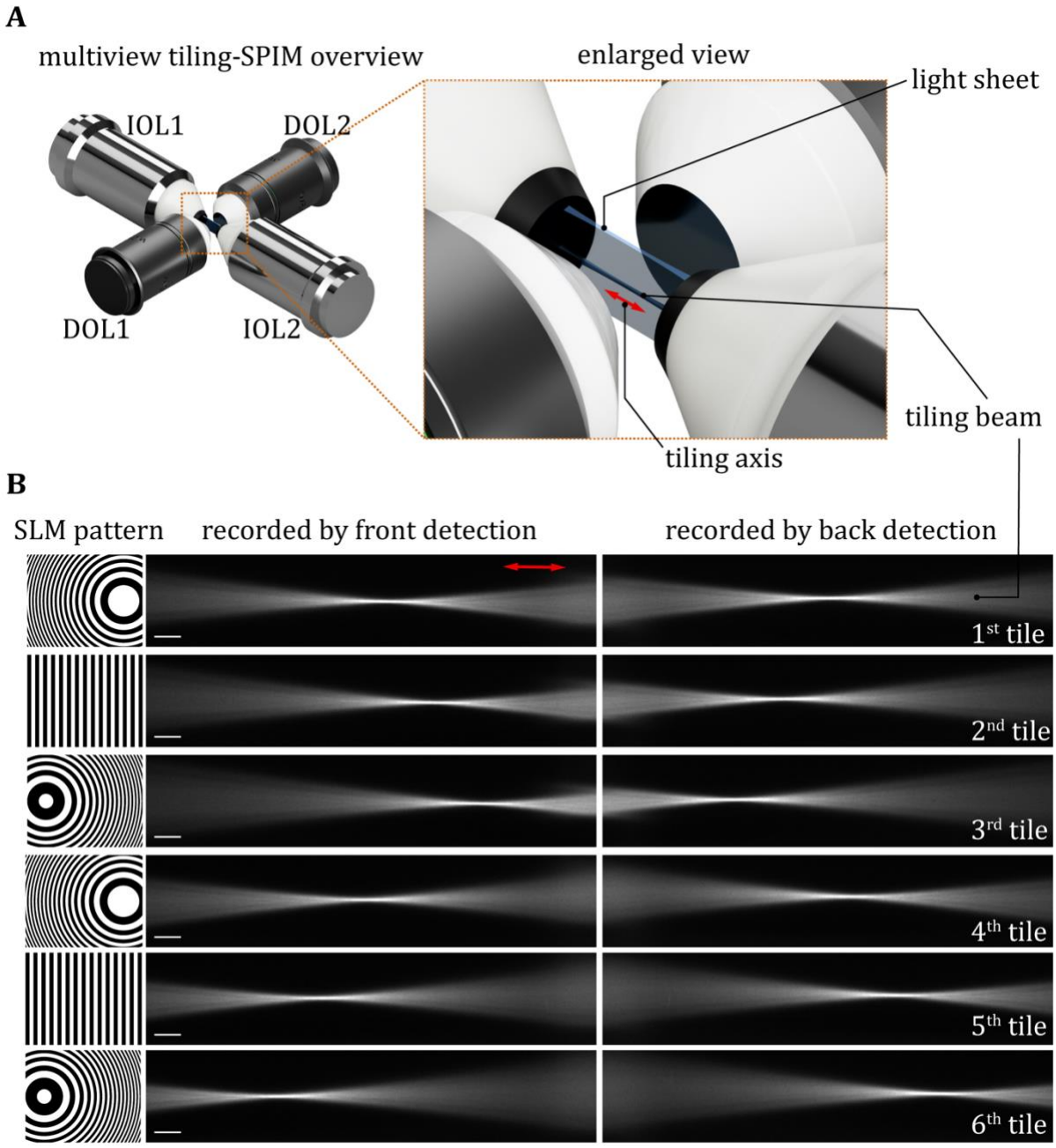

Fig. S4. The tiling technique is depicted based on the Multiview-SPIM setup. (A) The Multiview-SPIM configuration with four objective lenses; two illumination objective lenses (IOL) and two detection objective lenses (DOL). (B) The left column depicts six distinct SLM patterns based on virtual lenses with various focal lengths, and the two right columns depict the recorded tiled illumination beams via two detection arms simultaneously. Scale bars, 20 μm.

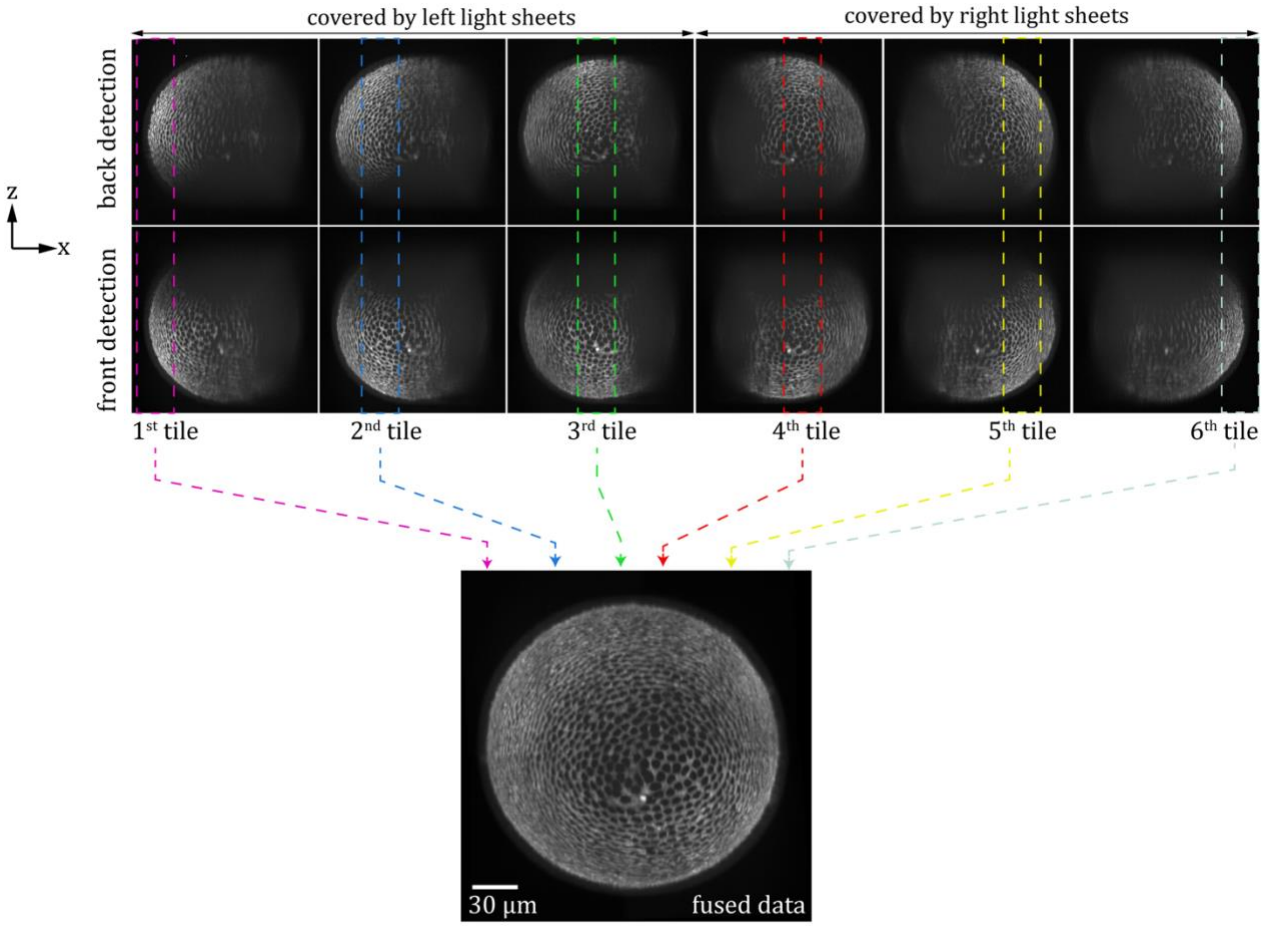

Fig. S5. The performance of the MT-SPIM for imaging an opaque sample (A) The recorded data with MT-SPIM by six tiles is composed of 12 volume images per single time point which are illuminated with multi-tiled light sheets and recorded from multi views. All views show axial views of the raw imaged based on maximum intensity projection (MIP) and each part of the sample that is illuminated with the particular tiled light sheet is indicated with color-coded dashed boxes. (B) The MIP of the reconstructed axial view.

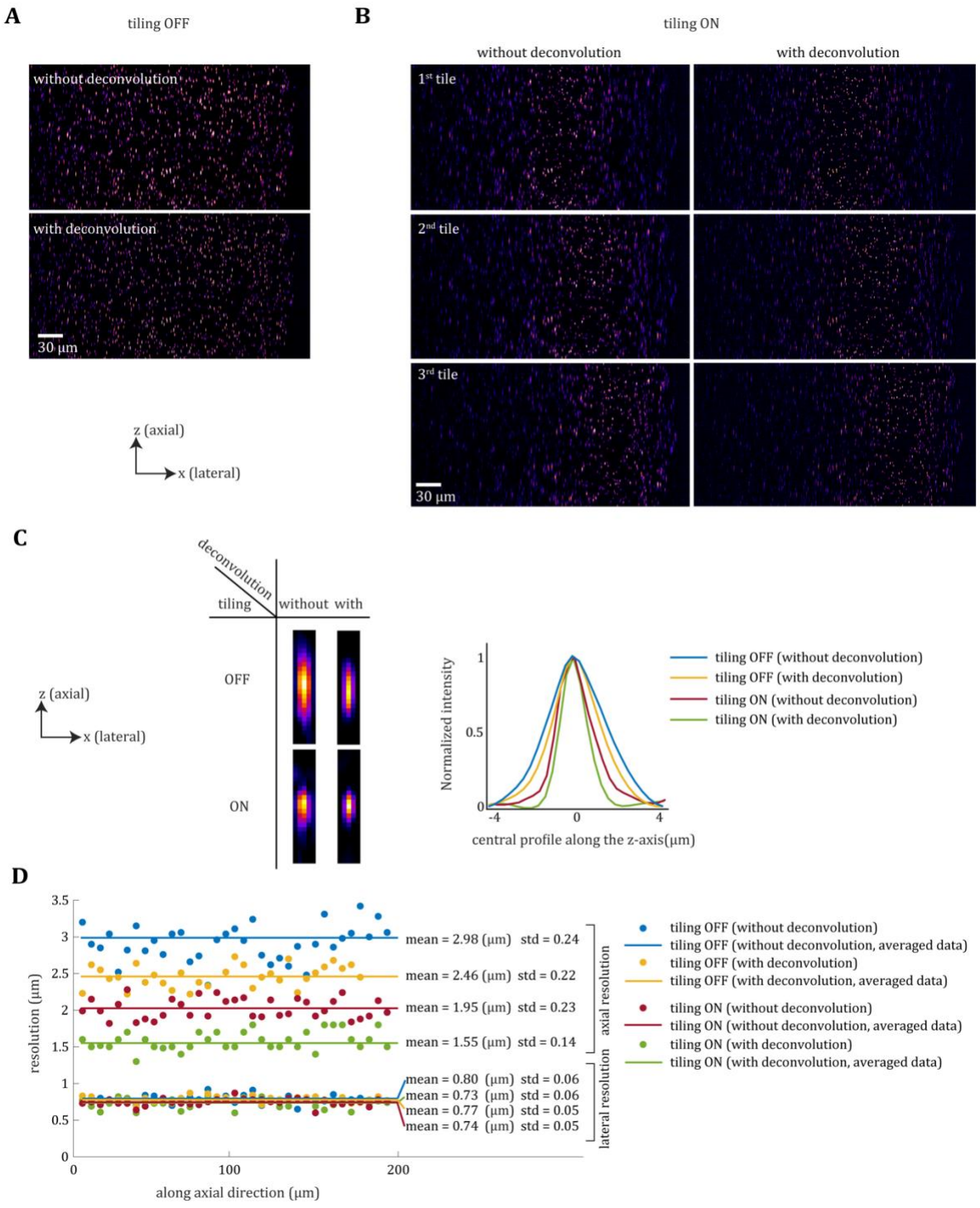

Fig. S6. SPIM experimental point spread function measurement comparing non-tiling SPIM vs tiling SPIM. The axial resolution of the microscope was determined by imaging 400 nm diameter fluorescent microspheres. (**A**) The axial view of microspheres imaged in the non-tiling SPIM mode. (**B**) The axial view of the microspheres imaged by the tiling SPIM mode. (**C**) An enlarged image of one of the imaged microspheres in two modes, as well as with and without deconvolution. The right plot depicts the center axial intensity distribution of the left images. (**D**) This graph summarizes the full width at half maxima of the microspheres (n=30) across 200 μm along the axial and lateral axes.

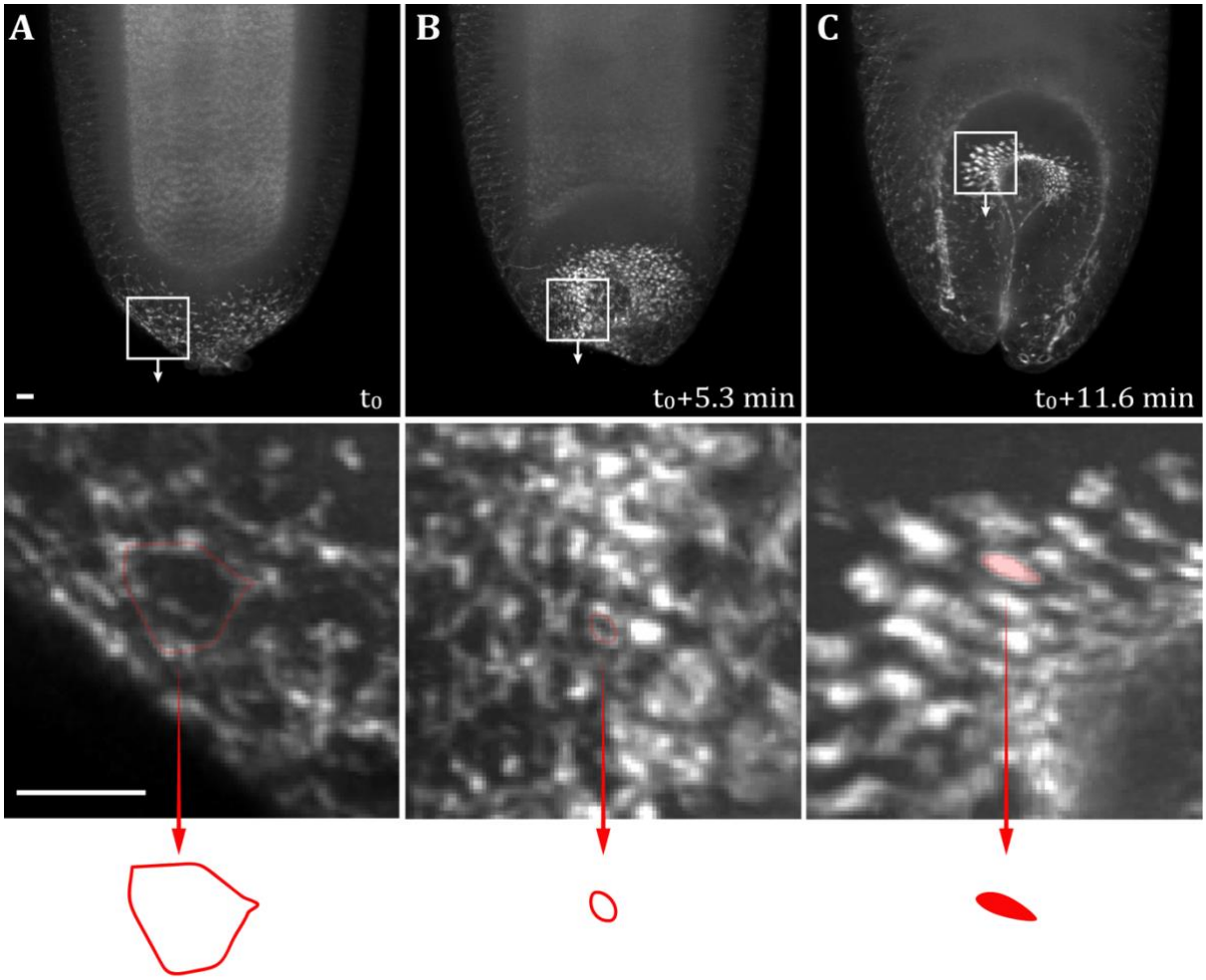

Fig. S7. Imaging of subcellular MyoII dynamics during posterior midgut invagination. Whole embryo volume imaging data were cropped to depict the dorsal posterior region of the embryo during posterior midgut invagination in a maximum intensity projection. (**A**) The initial phase of posterior midgut invagination is characterized by an apical accumulation of MyoII-GFP punctae that associate with the apical junctions of the cells in the posterior midgut primordium. (**B**) The MyoII-GFP punctae associated into ring-like structures within the apical areas of the cells in the primordium. (**C**) Further into posterior midgut invagination, additional MyoII-GFP aggregates form in the apical area of adjacent cells located in an anterior direction to the midgut primordium. Scale bars, 10 µm.

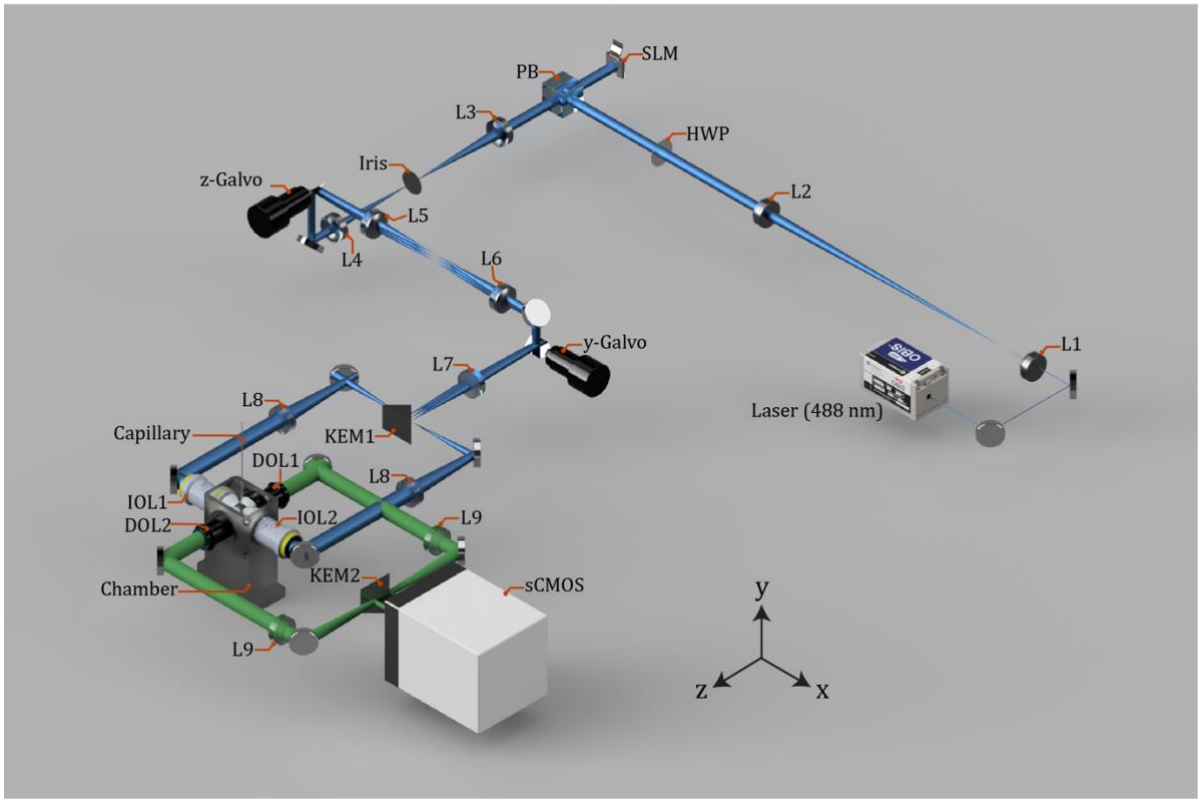

Fig. S8. Schematic of the MT-SPIM setup. The microscope includes two main optical arms: illumination and detection arm which are indicated with blue and green color. Within the illumination arm, a diode laser with 488nm wavelength operates as an illumination source to excite the green fluorescent protein (GFP) based sample. The optical beam's output diameter from the laser source is about 1 mm. It is not sufficient to interact with the spatial light modulator (SLM) with a diameter of around 12 mm. Hence, the optical beam is expanded to 12 mm diameter with two lenses telescope configuration (L1: 25 mm, L2: 300 mm) to cover the SLM area for an effective beam shaping. The light reflected from the SLM is passed through a lens (L3: 75 mm), creating a Fourier diffraction pattern. A pinhole filters the unwanted diffraction pattern caused by the inherent pixelated SLM's structure. The filtered light is then collected by another lens (L4: 75 mm) after an Iris pinhole to conjugate the pattern projected by the SLM. The conjugated illumination light heats the serial of optical elements such as a z-Galvo mirror, pair of two lenses (L5: 75 mm and L6: 75 mm), a y-Galvo mirror, and a transformer lens (L7: 75 mm). The z-Galvo mirror is used to reposition the illumination light through the sample for volume imaging which is conjugated using the pair lenses to the place of the y-Galvo mirror to produce the light sheet. The primary light sheet is detectable in the focal length of the transformer lens that is parked in front of the y-galvo mirror. The primary light sheet is faced with a knife-edge mirror (KEM 1) to send the light sheet into the right and left arm of the illumination beam for two side illuminations. The primary light sheet is then collected with the assembly of a lens (L8: 150 mm) and an illumination objective lens (IOL1 or IOL2, 10x Nikon water immersion) to deliver the light sheet to a specific layer of the sample. In the optical detection arms, which are indicated with green color, the emitted light from the sample is detected by two objective lenses (DOI1 and DOL2, 20x Olympus) simultaneously. In the final step, to record the image, the DOLs collect the signals from the sample and send them to a single sCMOS camera (V2 Orca-flash, Hamamatsu) which is combined by two tube lenses (L9: Olympus, 200 mm) and a knife-edge mirror (KEM 2) for simultaneous Multiview imaging.

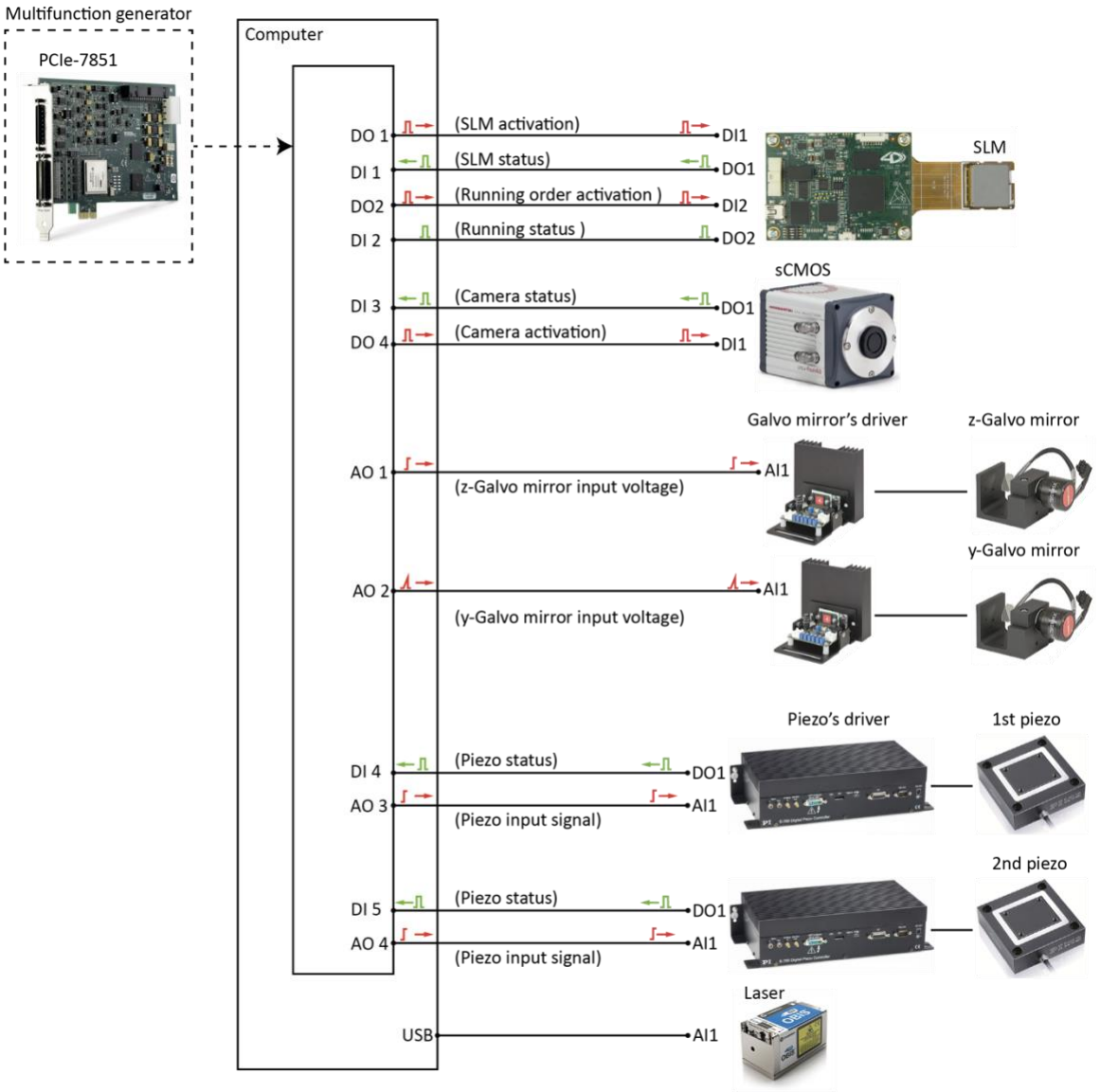

Fig. S9. Electronic structure of the MT-SPIM. The figure shows the architecture of the electronic connections between the components. A fast-programmable gate array (FPGA, PCIe-multifunction generator) is hosted for realtime signal controlling to have high-speed imaging. The electronic components are connected to the FPGA board with several digital and analog connections, which are indicated in the figure by digital input and digital output (DI and DO). All of the DI ports in the FPGA board operate parallel to monitor each component's status at the same time. The DO ports are also employed as emitter to send the command signal to each electronic part for a particular operation. In addition, the FPGA's analog output ports (AO) produce the analog electrical waveform for the component which are running based on the analogue signal such as scanning mirrors and piezoelectrics.

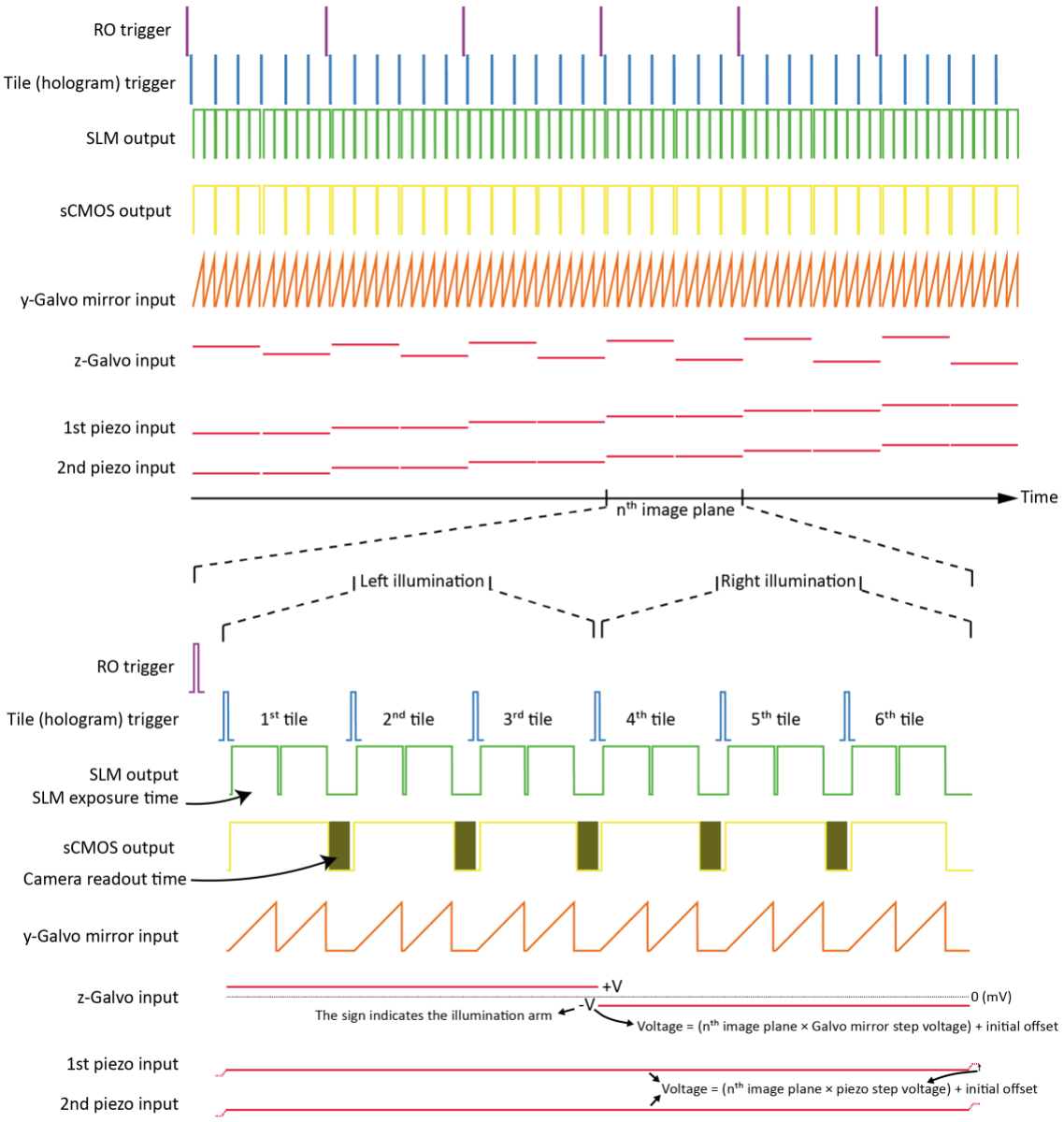

Fig. S10. The timing diagram of the MT-SPIM's electrical waveforms. All components operate based on predefined electrical waveforms. For each tiled light sheet the spatial light modulator (SLM) operates as a master clock, which is synchronized with camera exposure time. When the camera starts to collect the emitted light, the y-Galvo mirror is started to scan the illumination beam with a sawtooth wave to generate the light sheet. For the three tiled light sheets, the SLM, camera, and y-Galvo mirror operate simultaneously three times per illumination arm. All tiled light sheet illuminates a particular imaging plane which is tuned in the focus of the detection lens by the z-Galvo mirror with a constant voltage. After one complete illuminated arm, the three tiled light sheet switches to the second illumination arm by changing the z-Galvo mirror's voltage by a negative sign. In addition, in the detection side, to keep the detection objective lenses in focus for all tiled light sheet, the voltage of the piezos is settled constant during the imaging of a single plane. After that, piezoes' voltage are changed smoothly with a predefined step voltage to move the detection objective lenses to the next plane for 3D imaging.

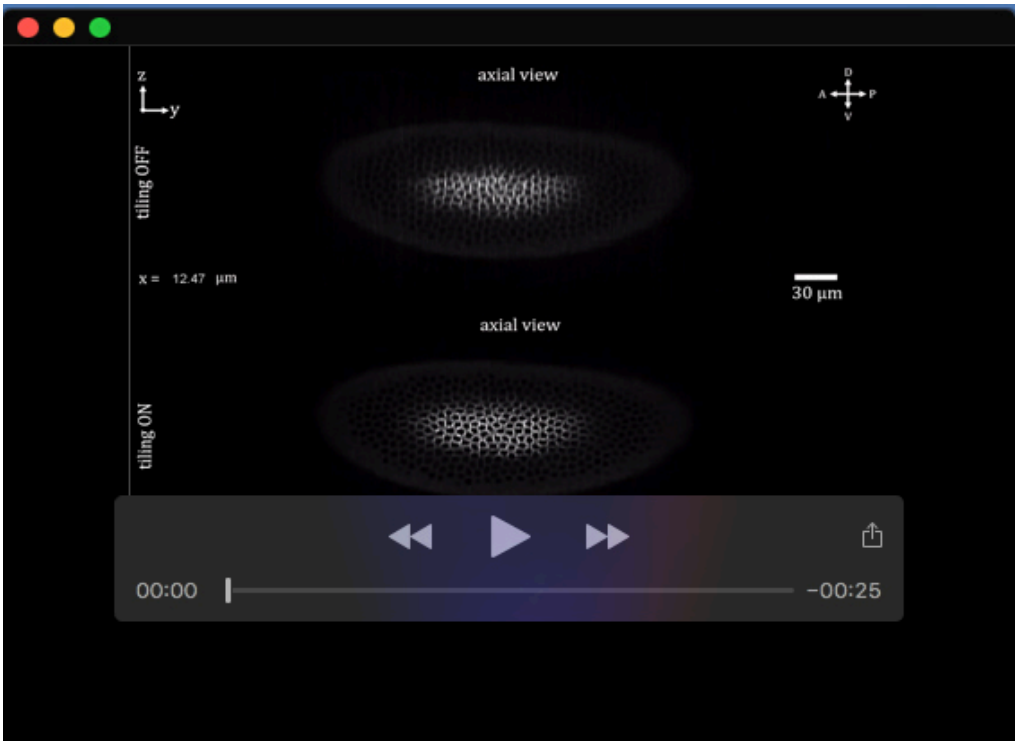

Movie 1. Comparison of the reconstructed axial images recorded by M-SPIM and MT-SPIM.

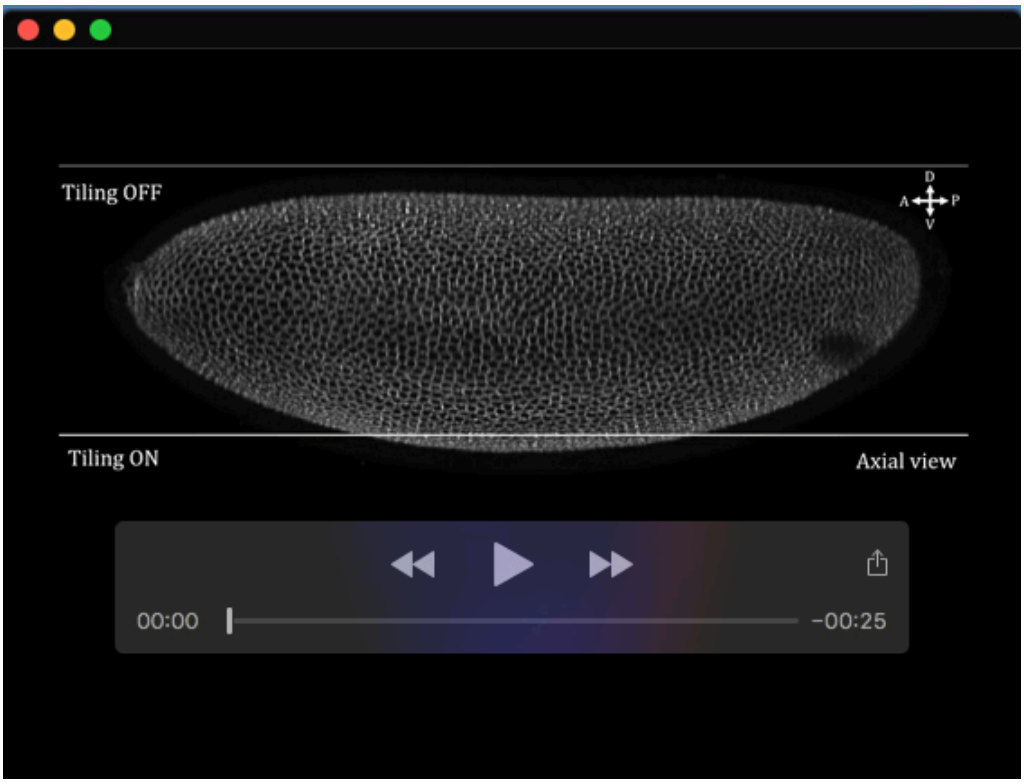

Movie 2. Maximum intensity projection of the reconstructed axial images recorded by MT-SPIM versus M-SPIM.

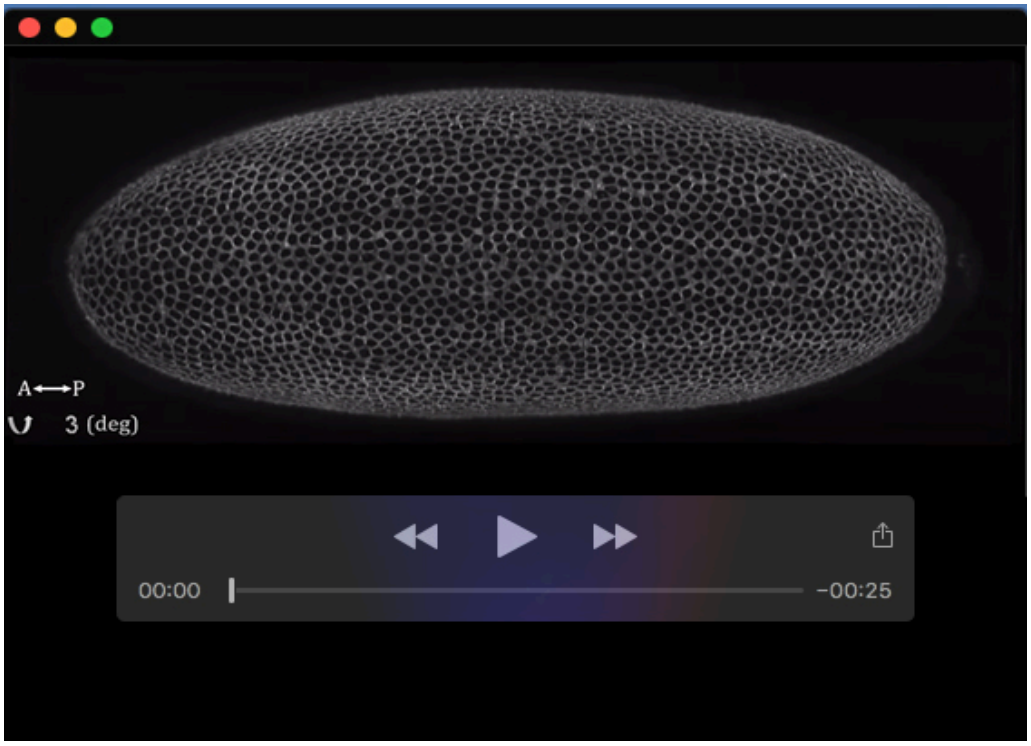

Movie 3. 3D rendering of a live Drosophila embryo image recorded by MT-SPIM at the start of the cellularization process.

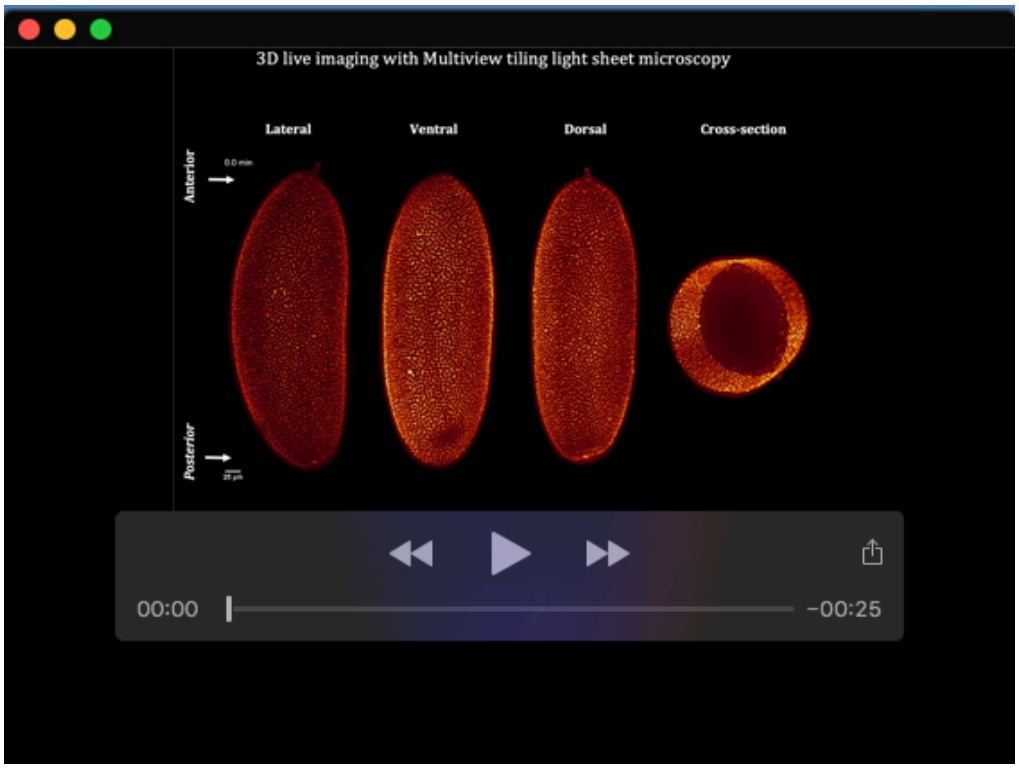

Movie 4. 3D visualization of a live *Drosophila* embryo recorded by the MT-SPIM during cellularization and the early stages of gastrulation.

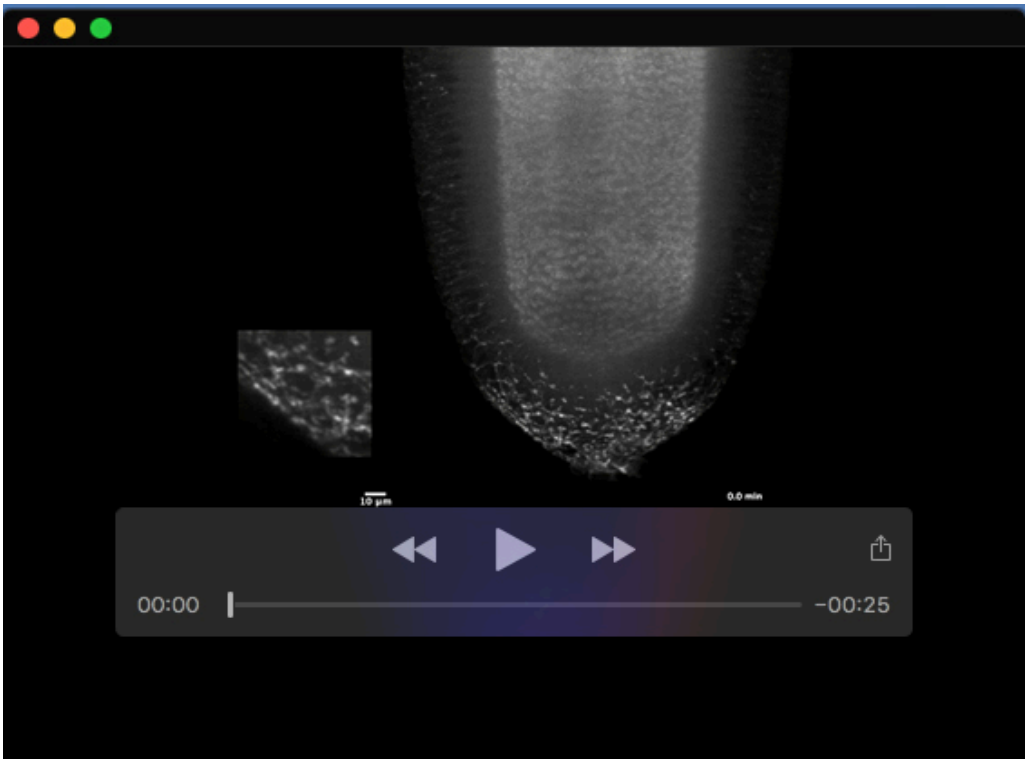

Movie 5. 3D rendering of a recorded live *Drosophila* embryo captured by the MT-SPIM during posterior midgut formation.

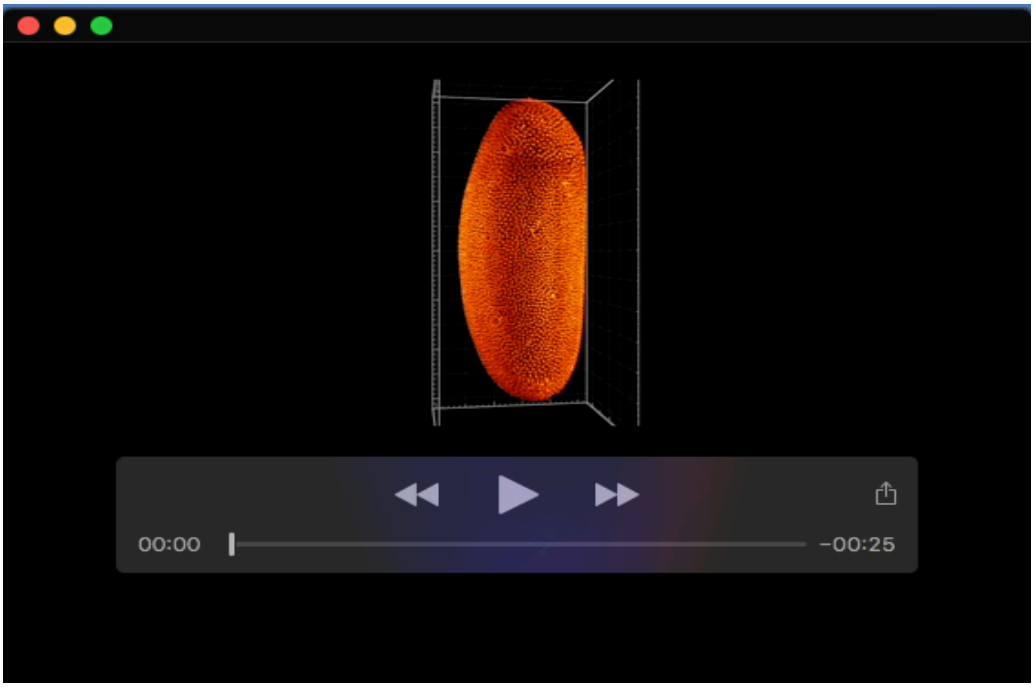

Movie 6. 3D rendering of a recorded live *Drosophila* embryo captured by the MT-SPIM during cellularization and early gastrulation compared to the M-SPIM.